

3-6-2009

Interfacial energy between carbon nanotubes and polymers measured from nanoscale peel tests in the atomic force microscope

Mark C. Strus

Purdue University - Main Campus, mstrus@gmail.com

Camilo I. Cano

Purdue University - Main Campus, CCano@Pactiv.com

R. Byron Pipes

Purdue University - Main Campus, bpipes@purdue.edu

Cattien V. Nguyen

NASA Ames Research Center, cattien.v.nguyen@nasa.gov

Arvind Raman

Purdue University - Main Campus, raman@purdue.edu

Follow this and additional works at: <http://docs.lib.purdue.edu/nanodocs>

 Part of the [Applied Mechanics Commons](#), [Nanoscience and Nanotechnology Commons](#), and the [Polymer and Organic Materials Commons](#)

Strus, Mark C.; Cano, Camilo I.; Pipes, R. Byron; Nguyen, Cattien V.; and Raman, Arvind, "Interfacial energy between carbon nanotubes and polymers measured from nanoscale peel tests in the atomic force microscope" (2009). *Other Nanotechnology Publications*. Paper 164.

<http://docs.lib.purdue.edu/nanodocs/164>

This document has been made available through Purdue e-Pubs, a service of the Purdue University Libraries. Please contact epubs@purdue.edu for additional information.



Interfacial energy between carbon nanotubes and polymers measured from nanoscale peel tests in the atomic force microscope

Mark C. Strus^a, Camilo I. Cano^b, R. Byron Pipes^{b,c,d}, Cattien V. Nguyen^e, Arvind Raman^{a,*}

^a Birck Nanotechnology Center and School of Mechanical Engineering, Purdue University, West Lafayette, Indiana, USA

^b School of Chemical Engineering, Purdue University, West Lafayette, Indiana, USA

^c School of Aeronautics and Astronautics, Purdue University, West Lafayette, Indiana, USA

^d School of Materials Engineering, Purdue University, West Lafayette, Indiana, USA

^e ELORET Corp, NASA Ames Research Center, Moffett Field, California, USA

ARTICLE INFO

Article history:

Received 20 December 2008

Received in revised form 17 February 2009

Accepted 19 February 2009

Available online 6 March 2009

Keywords:

A. Nanoscale peeling

B. Carbon nanotubes

C. Polymer nanocomposites

D. Interfacial fracture energy

E. Atomic force microscope

F. Surface energy

ABSTRACT

The future development of polymer composite materials with nanotubes or nanoscale fibers requires the ability to understand and improve the interfacial bonding at the nanotube–polymer matrix interface. In recent work [Strus MC, Zalamea L, Raman A, Pipes RB, Nguyen CV, Stach EA. Peeling force spectroscopy: exposing the adhesive nanomechanics of one-dimensional nanostructures. *Nano Lett* 2008;8(2):544–50], it has been shown that a new mode in the Atomic Force Microscope (AFM), peeling force spectroscopy, can be used to understand the adhesive mechanics of carbon nanotubes peeled from a surface. In the present work, we demonstrate how AFM peeling force spectroscopy can be used to distinguish between elastic and interfacial components during a nanoscale peel test, thus enabling the direct measurement of interfacial energy between an individual nanotube or nanofiber and a given material surface. The proposed method provides a convenient experimental framework to quickly screen different combinations of polymers and functionalized nanotubes for optimal interfacial strength.

Published by Elsevier Ltd.

1. Introduction

Carbon nanotubes (CNTs) are gaining significant interest as nanoreinforcements for strong, durable, lightweight polymer composite materials due to their unusually high tensile and compressive modulus [2,3]. When properly dispersed in a polymer matrix material, CNTs could allow for improvement in fracture toughness and fatigue properties since the CNT size is on the same order as defects in the material [4]. Many researchers have shown that the addition of a small volume fraction of CNTs to various polymers can improve the bulk modulus of the composite materials such as epoxy [5], polyimide [6], polyethylene [7], methyl-ethyl ethacrylate [8], or polyvinyl alcohol [9]. Additionally, the large electrical and thermal conductivities of carbon nanotubes have led to the creation of unique nanocomposites that can quickly dissipate electrostatic charges [10] or withstand high temperatures with minimal mechanical degradation [11]. Since the first reported work on CNT-reinforced polymer nanocomposites materials [12], they have found widespread application in automotive, aerospace, defense, sporting goods, infrastructure, and medical sectors [13–15].

However, the advancement of CNT nanocomposites has been hindered, among other things, by the lack of understanding of the interfacial bonding between CNTs and the surrounding matrix [16]. Better interfacial strength, especially shear strength, is impor-

tant to improve the nanocomposites bulk properties [17]. However, to date, only a few techniques [18–20] are able to directly measure the interfacial fracture energy between an individual CNT/nanofiber and surrounding matrix despite recent calls for individual fragment, pulling, and peeling experiments between polymers and CNTs/nanofibers [4].

In this work, we show how the recently developed peeling force spectroscopy using an atomic force microscope (AFM) [1] is capable of *quantitatively* comparing the interfacial fracture energy between multi-walled carbon nanotubes and different polymer materials. Through a continuum-based model of carbon nanotubes on graphite, we demonstrate how the interfacial and flexural energies acquired during peeling of a nanotube off a surface can be decoupled to find both the interfacial fracture energy (mode I fracture) between the nanotube and surface, as well as the flexural rigidity of the nanotube from a single force–distance curve in the AFM. We reveal experimental multi-walled CNT peeling results carried out with an AFM on substrates of graphite, epoxy, and polyimide. Based on hundreds of peeling experiments, we directly compare the interfacial energies between the CNTs and the different substrates representing typical polymer matrix materials for nanocomposites. The results show that peeling force spectroscopy is a promising tool that could be extended to compare, for example, the effects that specific matrix polymerization or nanotube/nanofiber functionalization [21] has on interfacial energy and load transfer in nanoreinforced nanocomposites.

* Corresponding author.

E-mail address: raman@purdue.edu (A. Raman).

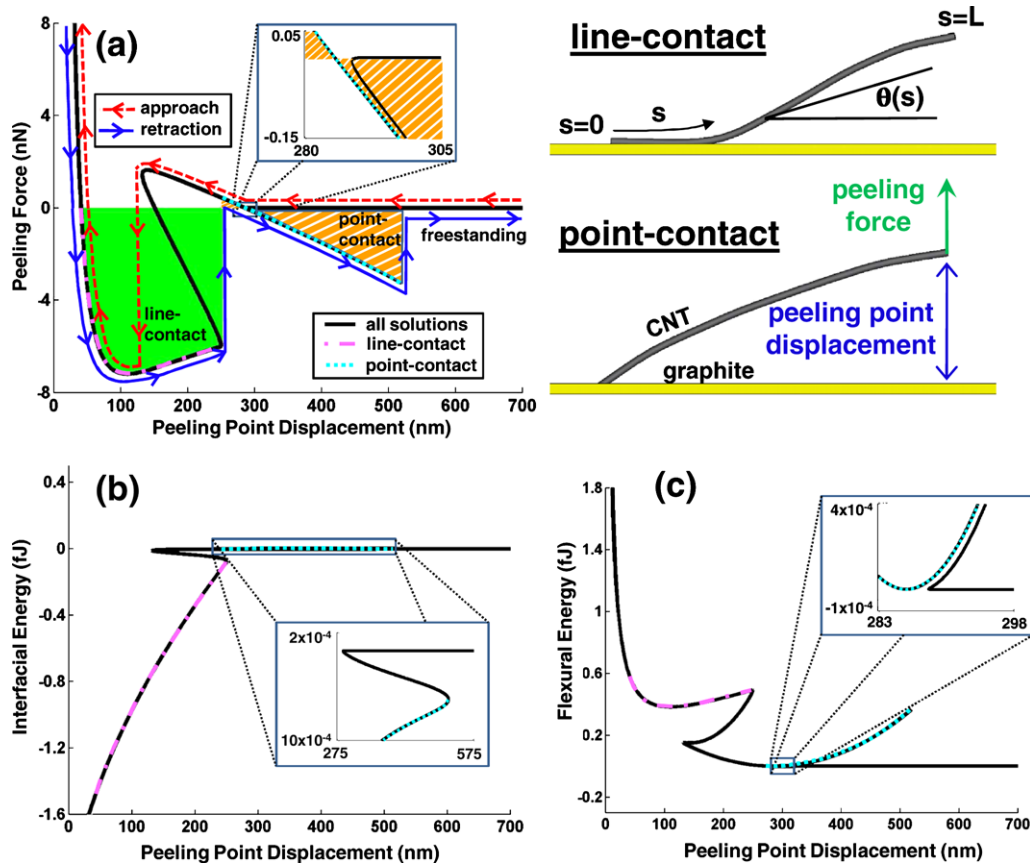


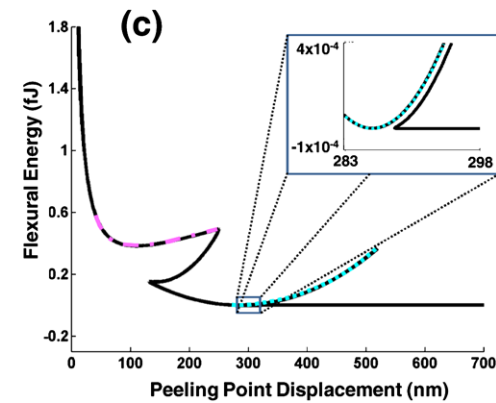
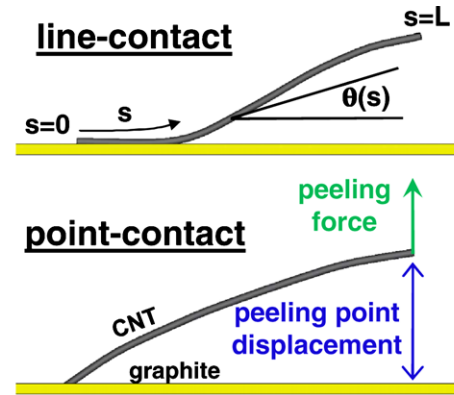
Fig. 1. Theoretically computed peeling of CNTs from graphite based on a computational model [1] using the inextensible elastica [26] for the CNT and Girafalco's universal graphitic potential for the CNT–surface interaction [23]. The solid black line in (a) shows all of the possible peeling forces as a function of the peeling point displacement with parameters representative of MWCNTs studied in the experiments: $L = 1.5 \mu\text{m}$, $E = 100 \text{ MPA}$, outer diameter $d_o = 41 \text{ nm}$, inner diameter $d_i = 10 \text{ nm}$, $I = \pi/64(d_o^4 - d_i^4)$. The dashed red and solid blue arrowed curves show the accessible forces that would be expected in an experiment as the CNT approaches and retracts from the surface. As the CNT is peeled off the surface, sudden force jumps occur as the CNT switches from a line-contact (dash-dotted magenta line) to a point-contact (dashed cyan line) to a freestanding configuration. The solid green and striped orange shaded areas under the respective line-contact and point-contact force–displacement curves during retraction represent the work added to the system by the external force that peeled the CNT. When the instantaneous interfacial (b) and flexural energies (c) are plotted as a function of peeling point gap, it is apparent that most of the work done during line-contact peeling changes the interfacial energy in the system while most of the work done during point-contact peeling changes the flexural energy in the CNT.

2. Theoretical basis of proposed method

We begin with a theoretical model of a CNT being peeled from a flat surface with specific interaction forces. In carbon nanotube nanocomposites, three types of CNT–polymer matrix interaction forces are relevant: micro-mechanical interlocking [16], chemical bonding [22], and van der Waals interaction forces. We study CNT peeling that takes into account the van der Waals interaction forces based on the universal graphitic potential [23]. However, the model can be extended to include chemical bonding which becomes important for functionalized CNTs [21] or mechanical interlocking [24]. The developed computational model, described in detail in Strus et al. [1] and Zalamea [25] is used here to demonstrate how different regions of peeling force–displacement measurements can be used to decouple and quantify both the interfacial energy and the flexural stiffness of the CNT.

2.1. Nanotube configurations during peeling: point- and line-contact

In the formulation, the CNT is modeled as a large deformation, continuum inextensible elastica [26] that interacts with a graphite surface via van der Waals interaction forces [23]. The resulting non-linear boundary value problem is solved numerically to find the peeling forces applied to the fixed end of the nanotube as a function of the crack opening or peeling point displacement between



the CNT and substrate (see Fig. 1a for a $1.5 \mu\text{m}$ multi-walled CNT with inner and outer diameters of 10 nm and 41 nm). As described in [1] and verified elsewhere [27], multiple solutions with differing forces and extensible elastica deformed shapes can exist for certain peeling point displacements (see Fig. 1a at peeling point displacement of 200 nm). However, in a typical peeling experiment the peeling probe will either approach or retract from the surface, thus allowing access only to some of the solution branches, as indicated by the dashed red¹ (approach) and solid blue (retraction) arrowed lines in Fig. 1a. In both approach and retraction of the CNT, the peeling force may suddenly drop or jump as the CNT switches from one equilibrium solution branch to another. Generally, the peeling force jumps, which are observed experimentally, indicate a sudden change in the deformed shape of the CNT.

In general, there are three forms of CNT deformed shapes during a peeling event. When a CNT is in a s-shape configuration [28], it forms a *line-contact* with the underlying surface as shown in Fig. 1 and thus interfacial adhesion is greatest during this stage of peeling. In the arc-shape configuration [28], the CNT only forms a *point-contact* and thus interfacial adhesion is small. Because the external applied force acts through a known distance, the area under the force–displacement curve indicates the amount of work in opening the peeling point or crack tip. In both line- and

¹ For interpretation of color in Fig. 1, the reader is referred to the web version of this article.

point-contact peeling, assuming small CNT–substrate friction [29] and negligible substrate deformation [30], the work of the applied peeling force either creates new nanotube and substrate surfaces (interfacial energy) or deforms the nanotube (flexural energy).

With the computational model, the instantaneous interfacial energy can be calculated as a function of the peeling point displacement as shown in Fig. 1b simply by integrating the CNT–substrate interaction forces per unit length along the length of the CNT such that

$$\text{Interfacial Energy} = \frac{EI}{L} \int_0^L f(z(s)) \sin \theta(s) ds \quad (1)$$

where E is the CNT flexural elastic modulus, I is its area moment of inertia, L is the CNT length, θ is the angle the CNT makes with the horizontal at every point along the length of the CNT, such that $s = 0$ at the free end, and $s = L$ and the peeling point. The interaction force between the CNT and graphite substrate results from the universal graphitic potential [23] acting at every point along the CNT and is shown simply as $f(z(s))$ (for details see [1]). The magnitude of the force depends on the distance z between the CNT and substrate.

Similarly, the flexural energy can be calculated as a function of peeling point gap,

$$\text{Flexural Energy} = \frac{EI}{2L} \int_0^L \left(\frac{d\theta}{ds}(s) \right)^2 ds \quad (2)$$

where $\frac{d\theta}{ds}(s)$ represents the radius of curvature along the CNT. The interfacial and flexural energies have been shown as a function of peeling point displacement in Fig. 1 for a 1.5 μm CNT peeled from a graphite surface. The portions of the energies corresponding to the line- and point-contact peeling events in Fig. 1a have been labeled accordingly. Recall that the total work of peeling is simply the sum of the change in interfacial energy plus the change in flexural energy.

2.2. Predicting interfacial energy from line-contact peeling

By understanding the interfacial and flexural energy contributions in the line-contact and point-contact configurations of the CNT, it becomes possible to extract the interfacial and flexural energies separately. When the CNT is peeled from the substrate in its line-contact configuration, Fig. 1b and c shows most of the work of peeling changes the interfacial energy in the system, while just a small amount goes into changing the flexural energy in the CNT. Therefore, the area under the line-contact portion of a peeling experiment can be used to approximate the change in interfacial energy.

During point-contact CNT peeling, the change in interfacial energy is negligible (see Fig. 1b), indicating that nearly all of the work done by the external peeling force is transferred into flexural deformations of the CNT. Thus, the slope of the arc-shape peeling force–displacement provides a good estimate of the CNT bending compliance, $c = L^3/3EI$. For the relatively stiff multi-walled CNT in Fig. 1, the peeling force–displacement slope in the line-contact peeling regime underpredicts the actual CNT flexural compliance by 10%. For less stiff single-walled CNTs, this flexural compliance approximation method becomes error prone.

The method to estimate interfacial energy change from the total work done during line-contact peeling is valid only for nanotubes or nanofibers with certain aspect ratios. Fig. 2 shows the ratio of the change in interfacial energy to the total work of peeling during line-contact peeling for various hollow single-walled CNTs and solid carbon fibers with different aspect ratios. When this ratio is near 100% it means that the work of peeling (area under the curve in the line-contact regime) can predict the interfacial energy be-

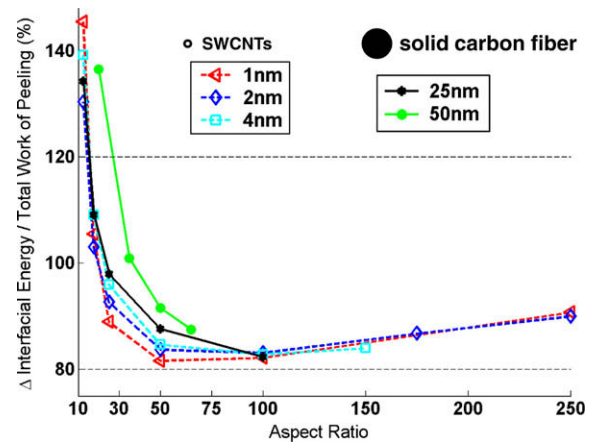


Fig. 2. Computationally-calculated percentage ratio of the change in interfacial energy to the total external work done during s-shape peeling for single-walled CNTs ($E = 1$ TPa) and solid carbon fibers ($E = 60$ GPa) on graphite as a function of length to diameter aspect ratio for different diameters. The data show there is a minimum aspect ratio around 15 for single-walled hollow CNTs and 15–30 for a hypothetical solid carbon nanotube (representing the limiting case of a multi-walled CNT) for which the change in interfacial energy can be approximated by the area under the peeling force–gap curve, which captures the total work added to the system. At smaller aspect ratios, the change in flexural energy is significant, and the approximation is invalid, though trends suggest the approximation should hold for nanoreinforcements with very large aspect ratios.

tween the CNT and the surface. This result will be the basis for the following experiments which quantitatively compare interfacial energies for different CNT–polymer substrate interactions.

3. Peeling experiments

3.1. Experimental setup

Dozens of multi-walled CNTs were attached to tipless microcantilevers from MikroMash™ and K-Tek Nanotechnology LLC™ as shown in Fig. 3, using a technique developed by Stevens et al. [31]. The attachment procedure is also described in our recent work [1]. Briefly, multi-walled CNTs, initially grown via chemical vapor deposition on a thin Pt/Ir wire, were properly aligned in a dark-field microscope and would naturally stick to the 10 nm thick nickel-coated tipless microcantilevers due to van der Waals forces. A voltage bias was applied to the microcantilever causing localized Joule heating at the point of highest resistance, the CNT–microcantilever interface, thus welding the CNT in place. In general, this CNT–microcantilever weld was strong enough to hold up for thousands of peeling experiments and the CNT would usually sever before the weld gave out.

Peel tests were carried out with in an Agilent 5500™ AFM system in a dry nitrogen chamber with near 0% relative humidity. The bending stiffness of tipless AFM microcantilevers were experimentally calibrated between 2 and 20 N/m using the method of Sader and Chon [32]. All of the experimental results presented here were completed with the two CNTs shown in Fig. 3 with an initial deviation from straightness <1% [33], although the observed phenomena were also repeatable with CNTs with larger deviation from straightness.

Besides highly order pyrolytic graphite, two polymeric substrates, polyimide (LaRC-1A) and epoxy adhesive (Cycom 7714A) were chosen as a representative thermoplastic and thermoset, respectively. N-methyl-2-pyrrolidinone (NMP) was obtained from Sigma–Aldrich™, while 4,4'-oxydiphthalic dianhydride (ODPA) and 3,4'-oxydianiline (ODA) were purchased from Chriskev Company Inc.™. The LaRC-1A precursor solution was prepared at room temperature by dissolving equimolar amounts of ODPA and ODA in NMP

(15% of solids by weight) in a round bottom flask equipped with a nitrogen blanket and mechanical stirring. This reaction was carried out for 24 h. All reagents were used as received. The polyimide substrate was obtained by spin coating a solution of the corresponding poly (amic acid) precursor solution (LaRC-1A) onto polished metal disks and letting it dry at 120 °C under vacuum for 48 h to reduce the NMP content as much as possible (some NMP will inevitably remain hydrogen bonded to the amic acid groups). After this drying step, the samples were put in a nitrogen-purged convection oven and the temperature was raised at a rate of 5 °C/min up to 300 °C and kept there for 2 h to guarantee full imide conversion. The slow heating rate was chosen to minimize void formation in the films during the imidization. Epoxy samples were prepared from B-staged resin dissolved in NMP then spin-coated on polish metal disks and left to dry at 120 °C for 48 h under nitrogen atmosphere. At the end of the drying stage, the films were completely cured and did not require any additional thermal treatment. A $5 \times 5 \mu\text{m}^2$ area of each sample was imaged with a conventional AFM probe to evaluate waviness and roughness. As shown in Fig. 4, both the graphite and polymer samples show negligible waviness while their line scans show height variations $\pm 5 \text{ \AA}$ over $5 \mu\text{m}$, well within the expected surface roughness of the multi-walled CNTs.

3.2. Peeling on graphite, epoxy, and polyimide substrates

Fig. 4 shows a typical static AFM peeling experiment, where CNT peeling forces are recorded as a function of peeling point displacement with probe A on graphite, epoxy, and polyimide substrates. From prior work [1], it is possible to separate the cantilever snap-in and pull-off (cantilever adhesion to substrate) from the CNT peeling (CNT adhesion to substrate) by noting the force hysteresis at the closest approach distance is the cantilever adhesion. Once the cantilever pulls off from the substrate the remaining force jumps correspond in sequence to (a) the transition from line to point-contact, (b) jumps between multiple point-contact states due to CNT imperfections and, (c) a final jump from point-contact to freestanding state.

From Fig. 4 it is clear that the peeling signatures using probe A (Fig. 3a) on graphite, epoxy, and polyimide substrates show qualitatively similar force jumps indicating a passage through the same sequence of CNT configurations. Quantitatively, there are important differences. Because the aspect ratios of the multi-walled CNTs used here are greater than 50, the theory developed earlier in this paper can be easily applied to these data. Accordingly, the *interfacial energy* between the multi-walled CNT and the substrate can be calculated from the shaded solid green² region under the line-contact regime as indicated in Fig. 4. As shown in Fig. 4b, some curve extrapolations are needed to identify and measure the correct area in the line-contact regime. Similarly, the slope of the force–distance curve in the point-contact regime provides a measure of the flexural compliance of the multi-walled CNT.

CNT peeling experiments showed good repeatability under the same operating conditions. In Fig. 5a, the interfacial energies of the multi-walled CNT of peeling probe A are plotted, based on experiments performed with the same probe at five different locations on each of the three substrates a total of 25 times per location. The data were processed according to Fig. 4 to obtain the area under the line-contact part of the curve, in order to estimate the interfacial energy in each peel test. As expected, measurements at the several locations on the same substrate show a small distribution in interfacial energies, while measurements on the various substrates are clearly separated because their interfacial energies

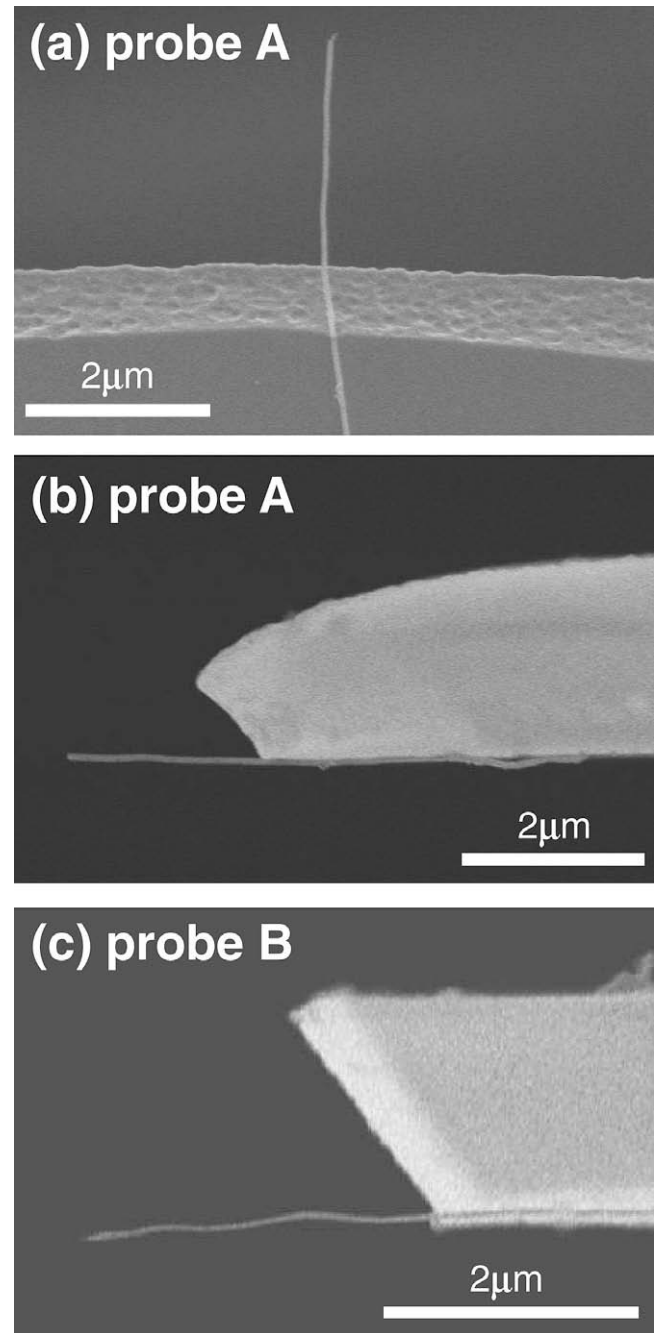


Fig. 3. Scanning electron microscopy images of the (a) bottom and (b) side of 2.2 μm long peeling probe A that was used to experimentally collect the data in Figs. 4 and 5a. The (c) side view of 2.5 μm peeling probe B used to collect the data in Fig. 5b. Statistical analysis of the CNT source using transmission electron microscopy revealed the CNTs used for the peeling probes have inner and outer diameters of $d_i = 10 \pm 2 \text{ nm}$ and $d_o = 40 \pm 6 \text{ nm}$.

are quite different. Therefore, the mean values of interfacial energies measured on each substrate can be used to quantitatively compare interfacial energies, so that CNT–epoxy is estimated to have an interfacial energy 1.5 times larger than CNT–graphite and 2.7 times larger than CNT–polyimide.

Fig. 5b shows a set of experiments completed with probe B where 20 peel tests were performed at 16 separate locations on both graphite and epoxy. The larger number of sample locations and fewer tests per location highlights the larger distribution of data particularly on epoxy. In this case, the mean epoxy/graphite interfacial energy ratio is 3.8, slightly larger than was

² For interpretation of color in Fig. 4, the reader is referred to the web version of this article.

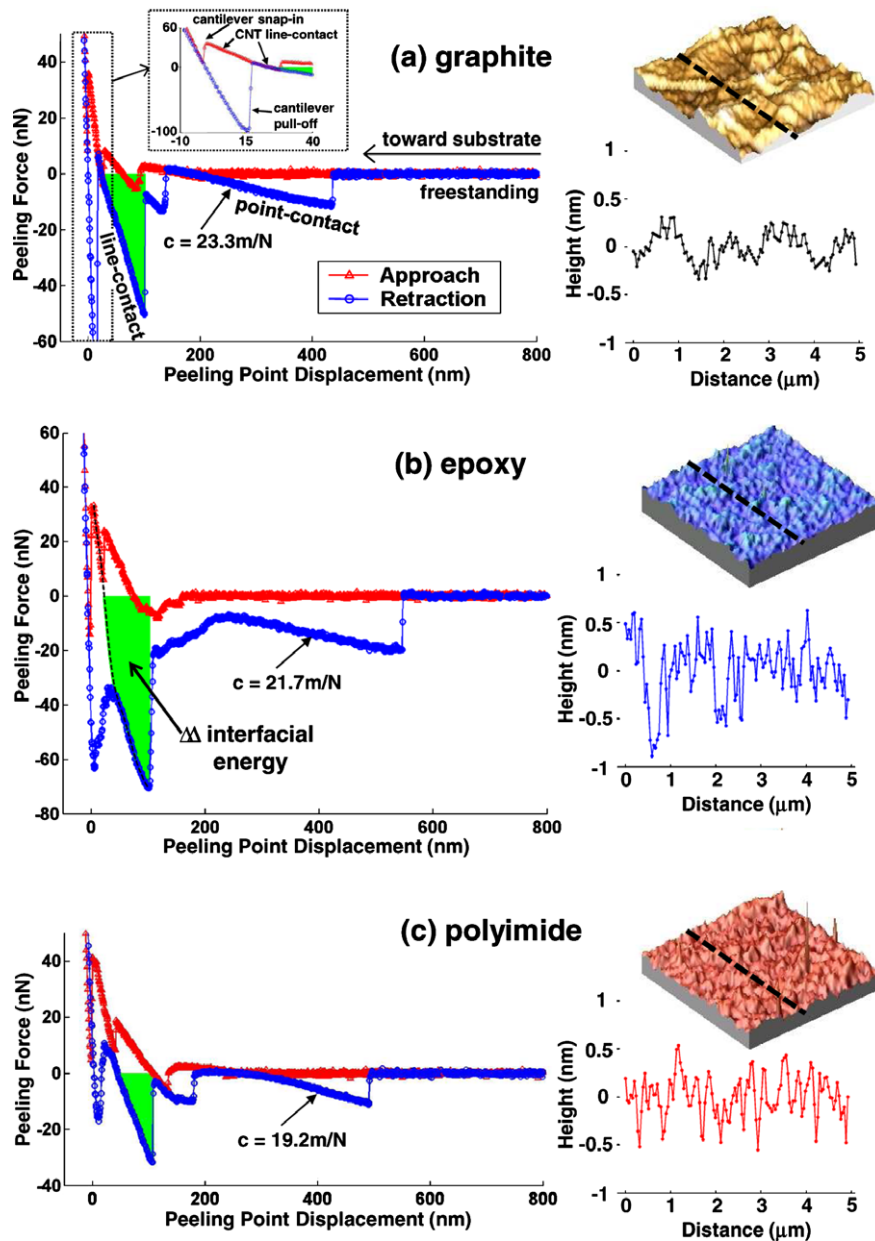


Fig. 4. Peeling force curves for probe A as a function of peeling point displacement on (a) graphite, (b) epoxy, and (c) polyimide. The approach and retraction force curves show the expected force jumps/drops predicted by the theoretical model as the CNT transitions between its line-contact, point-contact, and freestanding configurations. Additionally, all figures show the snap-in and pull-off for the AFM tipless microcantilever [1]. In the case of epoxy, a fourth-order polynomial (black-dashed line) has been fit to the line-contact portion of the approach and retraction curves because AFM microcantilever pull-off also pulled-off much of the CNT during retraction. In this way, the total work (shown to scale by the shaded solid green areas) during line-contact peeling could be compared on each substrate from the point where no external forces were acting on the CNT. Peeling curves on graphite and polyimide show an extra peeling event during retraction, which is likely due to defects which create non-uniform geometry or stiffness in the CNT. The slope of the point-contact peeling on all three surfaces is used to estimate the CNT's flexural compliance, c . AFM topography and line scan images show the small roughness values for each of the prepared surfaces. Height variations of 5 Å over 5 μm lengths are on the order of the CVD-grown multi-walled CNT roughness variations.

found with probe A. Although all experiments were carried out in a dry-nitrogen, adsorbed molecules or impurities such as amorphous carbon may contribute to the difference in interfacial energy ratios.

The proposed theory also suggests a recipe for measuring the flexural compliance of the nanotube from the point-contact regime of the experimental peeling force curve. In the Fig. 4, before the CNT transitions from point-contact to freestanding, the linear slope of each of the point-contact peeling curves can be used to estimate the CNT flexural compliance. Using this method, the CNT flexural compliance on graphite, epoxy, and polyimide is estimated to be

23.3 m/N, 21.7 m/N, and 19.2 m/N, respectively. These estimated compliances are similar on the three different substrates because only changes in flexural energy are expected during point-contact peeling. A similar theoretical compliance (22.6 m/N) could be achieved with $d_o = 55$ nm, $d_i = 10$ nm, $L = 2.2$ μm , and $E = 350$ GPa, all reasonable parameters for CVD-grown multi-walled CNTs.

These results clearly demonstrate how peeling force spectroscopy using an AFM can be used to measure the total interfacial energy during peeling (mode I fracture), and that the method clearly identifies the different interfacial energies between a given

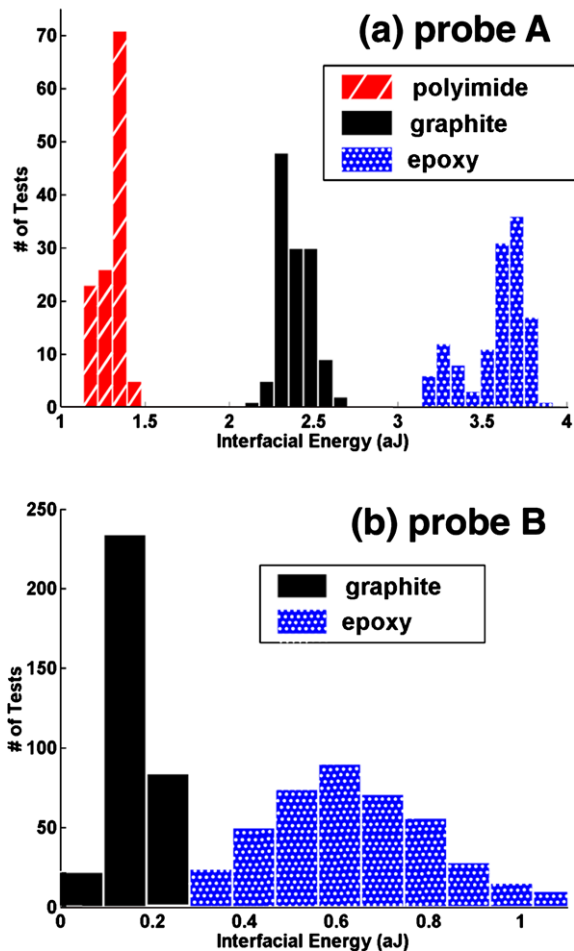


Fig. 5. Histograms showing the total interfacial energy calculated during line-contact peeling on various substrates. (a) Probe A was tested 25 times per location at five separate locations on graphite, epoxy, and polyimide substrates to clearly show their CNT–substrate interfacial energy differs. (b) Probe B was tested 20 times at 16 locations each on graphite and epoxy to demonstrate that the same CNT–substrate interfacial energy trend is observed with a different CNT.

nanotube and different polymer surfaces. Nonetheless, there are some important issues to keep in mind during such experiments:

- Interfacial energy ratios between substrates tested with the same probe on different days may vary because of substrate tilt relative to the CNT. Only mode I fracture/peeling (normal) is sensed by the microcantilever, but the CNT may also experience peeling in either mode II (friction-dominated) or mode III (lateral) type of crack opening, where sample tilt will play a significant role.
- Although the line-contact (immediately after cantilever pull-off) and point-contact (before return to freestanding) are readily recognized, additional force jumps are often observed (see Fig. 4a). These force jumps may either be additional line-contact peeling events, if the CNT was not initially well-adhered along its length, or point-contact events where the CNT tip geometry allows for sudden pivoting and/or slipping. Another possibility is the existence of a weak point in the CNT due to a defect, which leads to a sudden change in the overall bending stiffness of the CNT as it undergoes point-contact peeling.

Despite these challenges, these experiments have shown the clear measurement of CNT–epoxy and CNT–graphite interfacial energies with different probes and multiple trials demonstrating the robustness of the method.

4. Extracting interfacial fracture energy from peeling force spectroscopy

Although peeling force spectroscopy is very useful for readily comparing interfacial energies between nanotubes/nanofibers with different functionalizations and various polymers, the current experimental setup and accompanying model cannot provide interfacial energy per unit area, or interfacial fracture energy, for mode I fracture because the contact area of the CNT with the polymer substrate is unknown during s-shape peeling. Assuming full-length stiction of the CNT in Fig. 5a, one can obtain upper limit estimates of CNT–substrate interfacial energies per unit length on the three surfaces tested: 0.6 pJ/m for polyimide, 1.1 pJ/m for graphite, and 1.7 pJ/m for epoxy.

Though polyimide and epoxy are known to have similar free surface energies [34], the difference in their CNT–substrate interfacial energies may be due to local surface deformations during peeling, especially for epoxy, which generally has a lower bulk modulus [35,36]. In other words, if the measured interfacial energies were divided by a well-defined contact area, it is possible the CNT–substrate interfacial energy per unit area would be similar for these two polymers. Therefore, the reported interfacial measurements may depend both on the substrate’s surface and mechanical properties. Such is the case of graphite, which will deform little due to its large bulk modulus, but which shows a larger interfacial energy than polyimide because it has a much larger free surface energy [37]. Future improvements to AFM peel tests would benefit from inclusion of true contact length and area, perhaps by recent techniques where peeling experiments have been observed in a scanning electron microscope [38].

5. Conclusions

In this work, we have demonstrated the possibility of using nanoscale peeling with the AFM to quantitatively measure the interfacial bonding between nanotube–matrix interfaces in order to promote the development of stronger, tougher, and more robust nanocomposite materials. From an extension of previous work [1], we have shown that CNT peeling involves sudden transitions between different mechanical configurations or regimes (line-contact, point-contact and free standing). However, a key contribution was to identify that the force curves in different peeling regimes can be used to separate and quantify the interfacial energy and the flexural compliance of the CNT during the peeling process.

Using the proposed method, we have demonstrated through a series of peeling experiments, that CNTs have higher interfacial energies with epoxy than graphite, while CNTs and polyimides have the lowest interfacial energy of the three. This result clearly demonstrates the potential of the nanoscale peel test as a method of screening one-dimensional nanoreinforcement–matrix interfacial energies.

Before full acceptance as a screening tool, AFM peeling force spectroscopy requires improvements such as the elimination of sample tilt error, estimation of line-contact CNT adhesion contact area, the added ability to test nanotubes/nanofibers with large deviations from straightness and significant defects, and a better understanding of how mechanical properties measured at the polymer surface differ from those in the bulk configuration [39] where nanotube/nanofiber-reinforcements are typically added. Despite these shortcomings and in light of the few and often cumbersome alternatives [19,40], we have shown that the AFM peeling force spectroscopy method already offers the experimental ability to sensitively and quantitatively compare interfacial characteristics with minimal preparation, and will become a useful method for characterizing novel CNT/nanofiber functionalizations and

future polymerization techniques as the next generation of nanocomposites is developed.

Acknowledgement

This work was funded, in part, by the National Science Foundation through the Grant CMMI-0826356 “Cyber enabled predictive models for polymer nanocomposites: multi-resolution simulations and experiments,” and the Bilsland Dissertation Fellowship from the Purdue University graduate school. C.V.N is employed by ELORET Corporation at NASA Ames Research Center, and his work is supported by a subcontract from University Affiliated Research Center (UARC) operated by the University of California Santa Cruz at NASA Ames.

References

- [1] Strus MC, Zalamea L, Raman A, Pipes RB, Nguyen CV, Stach EA. Peeling force spectroscopy: exposing the adhesive nanomechanics of one-dimensional nanostructures. *Nano Lett* 2008;8(2):544–50.
- [2] Yu M-F, Lourie O, Dyer MJ, Moloni K, Kelly TF, Ruoff RS. Strength and breaking mechanism of multiwalled carbon nanotubes under tensile load. *Science* 2000;287:637–40.
- [3] Lourie O, Cox DM, Wagner HD. Buckling and collapse of embedded carbon nanotubes. *Phys Rev Lett* 1998;81:1638–41.
- [4] Desai AV, Haque MA. Mechanics of the interface for carbon nanotube–polymer composites. *Thin Wall Struct* 2005;43:1787–803.
- [5] Gojny FH, Wichmann MHG, Fiedler B, Schulte K. Influence of different carbon nanotubes on the mechanical properties of epoxy matrix composites – a comparative study. *Comp Sci Technol* 2005;65:2300–13.
- [6] Hu Y, Wu L, Shen J, Ye M. Amino-functionalized multiple-walled carbon nanotubes–polyimide nanocomposite films fabricated by in situ polymerization. *J Appl Polym Sci* 2008;110:701–5.
- [7] Ruan SL, Gao P, Yang XG, Yu TX. Toughening high performance ultrahigh molecular weight polyethylene using multiwalled carbon nanotubes. *Polymer* 2003;44:5643–54.
- [8] Velasco-Santos C, Martinez-Hernandez AL, Fisher F, Ruoff R, Castano VM. Dynamical-mechanical and thermal analysis of carbon-nanotube–methyl-ethyl ethacrylate nanocomposites. *J Phys D: Appl Phys* 2003;36:1423–8.
- [9] Coleman JN, Cadek M, Ryan KP, Fonseca A, Nagy JB, Blau WJ, et al. Reinforcement of polymers with carbon nanotubes. The role of an ordered polymer interfacial region. *Experiment and modeling*. *Polymer* 2006;47:8556–61.
- [10] Harris PJF. Carbon nanotube composites. *Int Mater Rev* 2004;49(1):31–42.
- [11] Wood JR, Zhao Q, Grogley MD, Meurs ER, Prins AD, Peijs R, et al. Carbon nanotubes: from molecular to macroscopic sensors. *Phys Rev B* 2000;62(11):7571–5.
- [12] Ajayan PM, Stephan O, Colliex C, Trauth D. Aligned carbon nanotube arrays formed by cutting a polymer resin–nanotube composite. *Science* 1994;265:1212–4.
- [13] Bal S, Samal SS. Carbon nanotube reinforced polymer composites – a state of the art. *Bull Mater Sci* 2007;30(4):379–86.
- [14] Hussain F, Hojjati M, Okamoto M, Gorga RE. Review article: polymer–matrix nanocomposites, processing, manufacturing, and application: an overview. *J Comp Mater* 2006;40(17):1511–75.
- [15] Breuer O, Sungararaj U. Big returns from small fibers: a review of polymer/carbon nanotube composites. *Polym Compos* 2004;25(6):630–45.
- [16] Wong M, Paramsothy M, Xu XJ, Ren Y, Li S, Liao K. Physical interactions at carbon nanotube–polymer interface. *Polymer* 2003;44:7757–64.
- [17] Andrews R, Jacques D, Qian D, Rantell T. Multiwall carbon nanotubes: synthesis and application. *Accounts Chem Res* 2002;25:1008–17.
- [18] Barber AH, Cohen SR, Wagner HD. Measurement of carbon nanotube–polymer interfacial strength. *Appl Phys Lett* 2003;82(23):4140–2.
- [19] Barber AH, Cohen SR, Kenig S, Wagner HD. Interfacial fracture energy measurements for multi-walled carbon nanotubes pulled from a polymer matrix. *Comp Sci Technol* 2004;64:2283–9.
- [20] Cooper CA, Cohen SR, Barber AH, Wagner HD. Detachment of nanotubes from a polymer matrix. *Appl Phys Lett* 2002;81(20):3873–5.
- [21] Salvatet J-P, Bhattacharyya S, Pipes RB. Progress on mechanics of carbon nanotubes and derived materials. *J Nanosci Nanotechnol* 2006;6:1857–82.
- [22] Frankland SJV, Caglar A, Brenner DW, Griebel M. Molecular simulation of the influence of chemical cross-links on the shear strength of carbon nanotube–polymer interfaces. *J Phys Chem B* 2002;106:3046–8.
- [23] Girifalco LA, Hodak M, Lee RS. Carbon nanotubes, buckyballs, ropes, and a universal graphitic potential. *Phys Rev B* 2005;62(19):103104–13110.
- [24] Schadler LS, Giannaris SC, Ajayan PM. Load transfer in carbon nanotube epoxy composites. *Appl Phys Lett* 1998;73(26):3842–4.
- [25] Zalamea L. On the cohesion of carbon nanotubes in nanostructures, PhD thesis, Purdue University, West Lafayette, Indiana, USA; 2007.
- [26] Love AEH. A treatise on the mathematical theory of elasticity. New York: Dover Publications; 1944.
- [27] Sasaki N, Toyoda A, Itamura N, Miura K. Simulation of nanoscale peeling and adhesion of single-walled carbon nanotube on graphite surface. *e-J Surf Sci Nanotechnol* 2008;6:72–8.
- [28] deBoer MP, Michalske TA. Accurate method for determining adhesion of cantilever beams. *J Appl Phys* 1999;86(2):817–27.
- [29] Lordi V, Yao N. Molecular mechanics of binding in carbon–nanotube–polymer composites. *J Mater Res* 2000;15(12):2770–9.
- [30] Yaltee RB, Young RJ. Evaluation of interface fracture energy for single-fibre composites. *Compos Sci Technol* 1998;58:1907–16.
- [31] Stevens R, Nguyen CV, Cassell A, Delzeit L, Meyyappan M, Han J. Improved fabrication approach for carbon nanotube probe devices. *Appl Phys Lett* 2000;77(21):3453–5.
- [32] Sader JE, Chon JWM. Calibration of rectangular atomic force microscope cantilevers. *Rev Sci Instrum* 1999;70(10):3967–9.
- [33] Deviation from straightness κ for a CNT was calculated from the side SEM image of a CNT. The CNT image was curve-fitted with a straight line, and the deviation from that line, ξ_n , was calculated for each point along the CNT. Then
$$\kappa = \sqrt{\sum \xi_n^2} / L_{CNT}.$$
- [34] Brandup J, Immergut EH, Grulke EA. *Polymer handbook*. 4th ed. New York: John Wiley and Sons, Inc.; 1999.
- [35] Yuen S-M, Ma C-CM, Chuang C-Y, Hsiao Y-H, Chiang C-L, Yu A, et al. Mechanical and electrical properties of TiO_2 coated multiwalled carbon nanotube/epoxy composites. *Compos Part A* 2008;39:119–25.
- [36] Yuen S-M, Ma C-CM, Chuang C-Y, Hsiao Y-H, Chiang C-L, Yu A, et al. Morphology and properties of acid and amine modified multiwalled carbon nanotube/polyimide composite. *Comp Sci Technol* 2007;67:2564–73.
- [37] Staszczuk P. Determination of water film pressure and surface free energy on graphite. *Mater Chem Phys* 1986;14:279–87.
- [38] Ishikawa M, Harada R, Sasaki N, Miura K. Visualization of nanoscale peeling of carbon nanotube on graphite. *Appl Phys Lett* 2008;93(6):083122.
- [39] Forrest JA, Dalnoki-Veress K. The glass transition in thin polymer films. *Adv Colloid Interface Sci* 2001;94:167–96.
- [40] Nuriel S, Katz A, Wagner HD. Measuring fibermatrix interfacial adhesion by means of a ‘drag-out’ micromechanical test. *Compos Part A* 2005;36:33–7.